Surface Reconstructions of Lamellar ABC Triblock Copolymer Mesostructures

N. Rehse,*,†,‡ A. Knoll,† R. Magerle,† and G. Krausch†,‡

Physikalische Chemie II and Bayreuther Zentrum für Kolloide und Grenzflächen, Universität Bayreuth, D-95440 Bayreuth, Germany

Received July 16, 2002

ABSTRACT: We show that the near surface structure of lamellar ABC triblock copolymer mesostructures can deviate considerably from the "ideal" surface anticipated from the bulk structure of the material. Varying the molecular architecture and the surface energy difference between the respective blocks, we show that such surface reconstructions are caused by a complex balance of enthalpic and entropic contributions to the free energy of the system. The results are compared to the well-known surface behavior of classical crystals and experimental conditions for what may be called "block copolymer surface science" are discussed.

1. Introduction

Microphase-separated block copolymers present a class of ordered materials,[1] which in many respects resemble crystalline matter. While the latter may be viewed as a three-dimensional periodic arrangement of atomic nuclei and electron density, an ordered block copolymer structure is a periodic array of polymer density. Despite the fact that the characteristic length scales differ by some 4 orders of magnitude, the search for similarities between the rather different types of ordered matter has repeatedly attracted scientific interest.[2−4] Examples are the determination and classification of the symmetry of the ordered mesophases, the characterization of defect structures and their thermal behavior, and certain routes of "single-crystal" preparation, such as the moving thermal gradient technique recently devised by Hashimoto and co-workers,[5] which closely resembles the zone melting procedure established for metal and semiconductor single-crystal preparation. An interesting similarity, which has not yet widely been investigated, concerns the *surface behavior* of ordered block copolymer samples. It is well-established in classical surface science that the absence of nearest neighbors can lead to significant deviations of the structure of the topmost atomic layer(s) of a crystal.[6] If only the lattice spacing perpendicular to the surface is changed, the effect of the surface is referred to as a "*surface relaxation*". If, in addition, the lateral arrangement of the atoms is affected by the surface, the effect is referred to as "*surface reconstruction*". Both relaxation and reconstruction can affect more than just the topmost atomic layer. The prominent example of the Si(111)7 × 7 reconstruction,[7] for example, is brought about by structural rearrangements (both laterally and perpendicular to the surface) of as much as the topmost five atomic layers.

The study of block copolymer surfaces dates back to the early 1980s when it was realized that irrespective of the underlying microdomain structure, the surface of diblock copolymer specimens is usually covered by the lower surface energy block.[8] Initiated by the thin film work of Anastasiadis et al.,[9] surface effects became an area of increasing interest at the beginning of the past decade, as they tend to dominate the morphology of block copolymer films in a thickness range of several bulk lamellar spacings.[10,11] Much of the work concentrated on lamella forming diblock copolymers, where the major effect lies in an alignment of the lamellae parallel to the confining surfaces. The more complex situation of ternary block copolymers has only recently been addressed both theoretically[12,13] and experimentally.[14−16] The first explicit comparison between structural effects on block copolymer surfaces and classical surface science was put forward by Stocker et al.,[14] who investigated the surface structure of an ABC triblock copolymer and interpreted the experimental findings as a surface reconstruction. Despite a constantly growing number of publications dealing with block copolymer thin films, an in-depth discussion of the observed effects in the light (and language) of classical surface science is still lacking. In a recent letter, we have started such a discussion based on experimental results on the near-surface structure of a lamellar ABC triblock copolymer forming a nonlamellar, reconstructed surface structure.[17] In the present publication, we present further experimental data on the surface behavior of the same and similar block copolymer systems. Furthermore, we work out in more detail the comparison between the effects found on the surfaces of block copolymer and the surface behavior of classical crystals. Our work is motivated by the conviction that similarities in the behavior of rather different classes of matter can reveal information on the underlying (general) concepts of nature.

The remainder of the paper is organized as follows. We first describe experimental results on the thin film and near-surface structure of four different ABC triblock copolymers, all of which exhibit a lamellar morphology in the bulk of the films (Figure 1). We then discuss the experimental results in view of the concepts established in classical surface science and try to identify similarities and differences of the surface behavior of these rather different classes of material.

* Corresponding author. E-mail addresses for all authors: nicolaus.rehse@uni-bayreuth.de; armin.knoll@uni-bayreuth.de; robert.magerle@uni-bayreuth.de; georg.krausch@uni-bayreuth.de.
† Physikalische Chemie II, Universität Bayreuth.
‡ Bayreuther Zentrum für Kolloide und Grenzflächen, Universität Bayreuth.

10.1021/ma021134v CCC: $25.00
Published on Web 04/03/2003

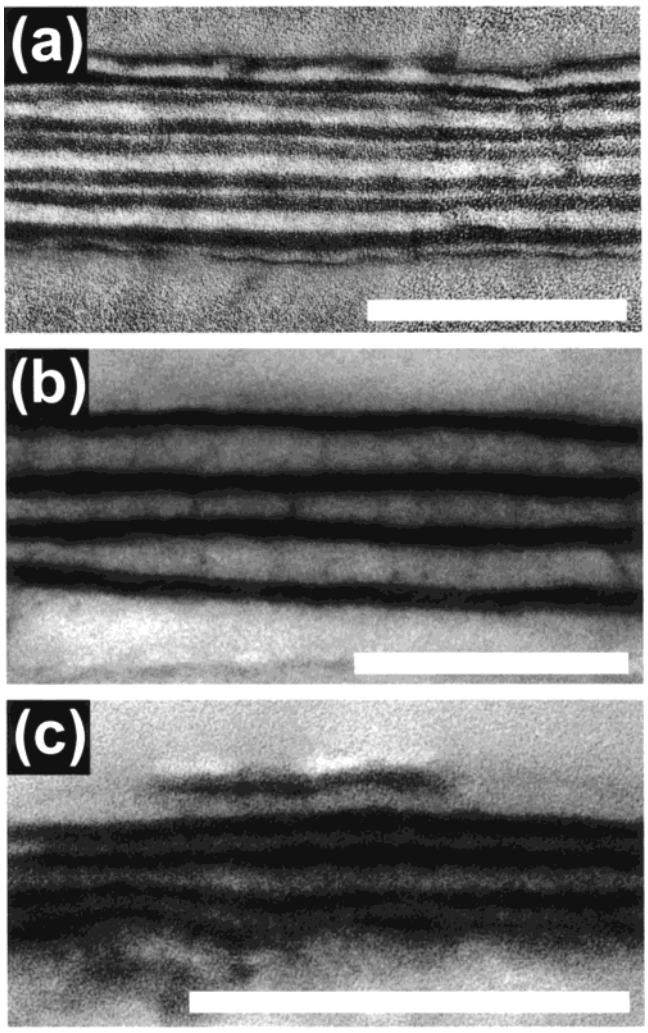

Figure 1. Cross sectional TEM images of thin films of SBM[162] (a), BSM[196] (b), and SBT[160] (c). All samples were stained with OsO_4; therefore, the dark regions can be assigned to PB. The scale bars represent 200 nm.

2. Experimental Section

Monodisperse batches of different linear triblock copolymers of the type polystyrene-*block*-polybutadiene-*block*-poly(methyl methacrylate) (SBM), polybutadiene-*block*-polystyrene-*block*-poly(methyl methacrylate) (BSM), and polystyrene-*block*-polybutadiene-*block*-poly(*tert*-butyl methacrylate) (SBT) were investigated in this study. All polymers were synthesized anionically following standard procedures.[18] Details concerning the synthesis and the bulk properties of the materials can be found in ref 19. The molecular parameters of the polymers are listed in Table 1. All four polymers exhibit a lamellar microstructure in the bulk. The characteristic lamellar spacing L_0 is included in Table 1.

Copolymer films of thickness 100−1000 nm were prepared on polished Si wafers by dip coating from 5 wt % polymer solutions in chloroform. To drive the samples toward thermodynamic equilibrium, the films were exposed to a well-controlled pressure of chloroform vapor (near but below saturation) for 1 day and dried slowly, by reducing the vapor pressure continuously over a period of 10 h. The samples were kept at a temperature $T_{sample} = 20.0 \pm 0.1$ °C in a closed vessel together with a chloroform reservoir kept at a slightly lower temperature $T_{solvent} = 19.5 \pm 0.1$ °C. The solvent vapor pressure was varied by variation of $T_{solvent}$. Care was taken to keep $T_{solvent} < T_{sample}$ to avoid infinite swelling of the polymer film and to ensure reproducible sample preparation. The preparation procedure resembles the solvent casting (slow drying) process typically used for bulk samples of these[19] and similar materials.

Table 1. Molecular Parameters of the Polymers Used in This Paper, Where M_w and M_w/M_n Are Determined by Size Exclusion Chromatography (SEC) Using a PS Standard)

polymer	M_w (kg/mol)	ϕ_{PS}	ϕ_{PB}	$\phi_{PMMA/PtBMA}$	M_w/M_n	L_0 (nm)
SBM[162]	162	0.33	0.47	0.20	1.02	∼80[a]
SBM[54]	54	0.34	0.37	0.29	1.04	47[b]
BSM[196]	196	0.35	0.35	0.30	1.12	105[b]
SBT[160]	160	0.32	0.35	0.33	1.04	85[b]

[a] For SBM[162], the characteristic bulk spacing L_0 was estimated based on the data provided in ref 38. [b] For the three remaining copolymers, the characteristic bulk spacing L_0 is taken from small-angle X-ray scattering (SAXS) experiments.[19]

The resulting thin film samples were investigated by optical microscopy (OM), TappingMode scanning force microscopy (SFM), cross sectional transmission electron microscopy (TEM), and low energy scanning electron microscopy (SEM). For the TEM experiments the films were floated off the SiO_x covered Si substrates onto aqueous KOH solution, picked up onto a TEM grid, embedded into epoxy, and subsequently cut into ∼50 nm thick slices. To avoid swelling in unreacted epoxy, the films were coated with a thin carbon layer prior to embedding. To enhance contrast the films were stained with OsO_4. For the SEM investigations RuO_4 was used as a selective stain. A field emission source with low energy electron beam (∼1 kV) was used. No further coating with a conductive material was needed.

3. Results

3.1. Surface Reconstructions. SBM. We start our discussion with the two SBM triblock copolymers. Prior to investigating the near-surface structure of the block copolymer, we have to unambiguously determine the "bulk structure" of our thin film samples. On the basis of the work on thin films of symmetric polystyrene-*block*-poly(methyl methacrylate) (SM) *di*block copolymers,[9,20] one expects an attraction of the polar M end block to the polar SiO_x substrate surface. In the diblock copolymer case, this attraction is known to lead to an alignment of the lamellae parallel to the plane of the film. To establish the "bulk structure" of the SBM triblock copolymer films, cross-sectional TEM images were taken. Figure 1a shows such an image for SBM[162]. One can clearly see the lamellar microdomain structure of the block copolymer aligned parallel to the plane of the film. The black regions can be assigned to PB, which is stained preferentially on exposure to OsO_4 vapor. According to the PMMA volume fraction, the thinner bright regions are assigned to PMMA. The wider bright regions are considered to be PS. The lamellar spacing $L_{0,film}$ amounts to 47 ± 5 nm and therefore is somewhat smaller than the bulk lamellar period $L_0 = 80$ nm (see Table 1). This deviation may be due to both beam damage on the PMMA[21] and some shrinkage of the film during the preparation process. The layered structure of the films is also reflected in SFM topography images of regions, where the film thickness is laterally varying. Here, the annealing process leads to the formations of areas of well-defined thickness (terraces),

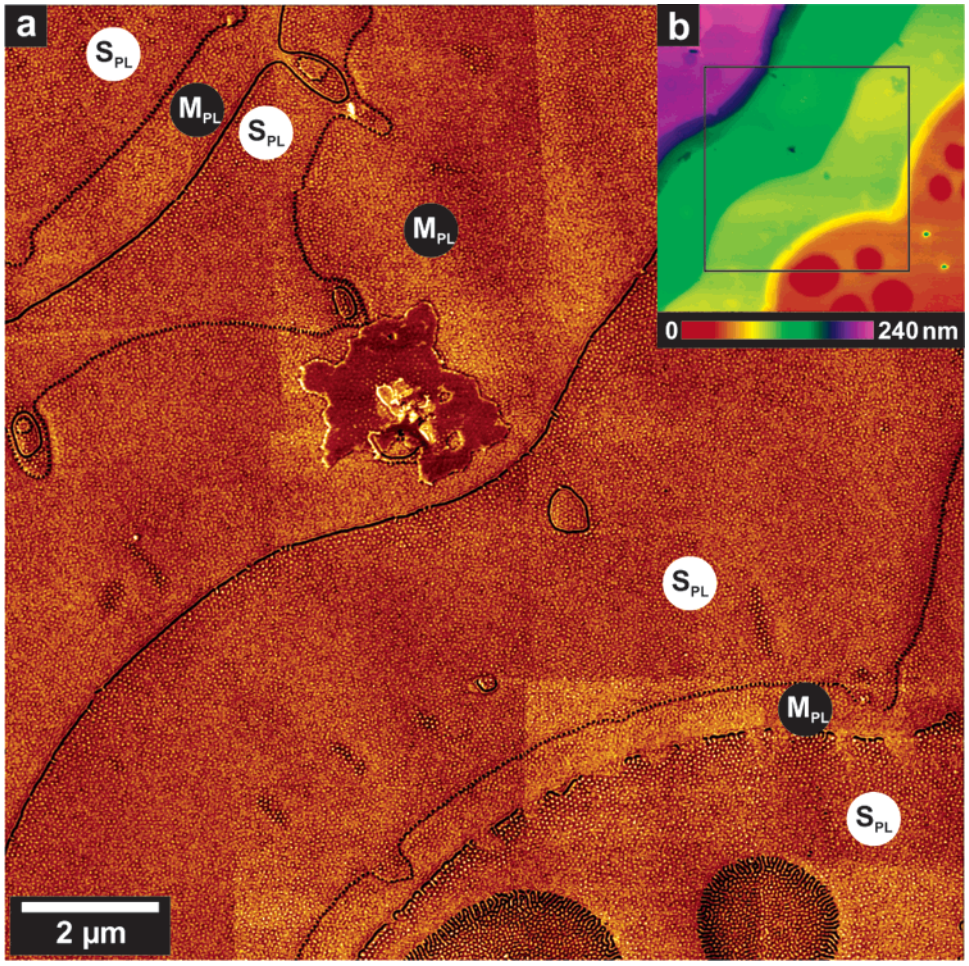

Figure 2. TappingMode SFM images of the phase contrast (a) and the topography (b) of the surface of a thin SBM[162] film. The phase contrast image corresponds to the black square in (b) and is a composite of 16 individual SFM images.

separated by steps of well-defined height H_{step} (Figure 2b). The terraced structure of the film surface is also found on spin-coated samples after solvent vapor annealing. So far the results closely resemble the behavior of diblock copolymer thin films. SFM measurements of the step heights H_{step}, however, yield values of only about half the lamellar period $L_{0,film}$ found in the bulk of the film ($L_{0,film} \approx 30$ nm). The absolute values are found to vary somewhat between different experiments. The relative values $H_{step}/L_{0,film}$, however, always follow the same trend, i.e., $H_{step} \approx {}^1/_2 L_{0,film}$. We note, though, that the determination of the lamellar spacing in the bulk of the film $L_{0,film}$ presents only a lower boundary to the actual value due to the beam damage on the PMMA blocks. In any case, we find that the step heights determined by SFM are always considerably smaller than the lamellar spacings determined from the cross sectional TEM images.

If the lamellar structure would proceed throughout the entire sample to the free surface of the film, a laterally homogeneous surface layer rich in one of the end blocks would be expected. However, higher resolution SFM images show unexpected lateral patterns on the terraces (Figures 2a and 3a). Two different types of lateral patterns are observed, which strictly alternate between successive terraces. For further reference and for reasons to become clear below, we refer to the two terrace structures as S_{PL} and M_{PL}, respectively. S_{PL} is characterized by isolated bright dots with a typical lateral repeat distance of some 60 ± 3 nm embedded in a continuous matrix. Terrace M_{PL} shows a similar pattern however with less contrast. Along with the terraces, the shape of the steps between them is found to alternate as well. As we move downward on the sample (from left to right in Figure 3a), the step from M_{PL} down to S_{PL} is continuous and rather featureless, while the step from S_{PL} down to M_{PL} has a dotted appearance in the SFM phase image.

To gain further insight into the near surface microdomain structure and to distinguish between the different materials we made use of the different etching rates of the three blocks in an oxygen plasma. The samples were exposed to an RF plasma in air (Harrick Plasma Cleaner, 1 mbar, 60 W at 13.56 MHz, 45 s). As determined from SFM measurements prior to and after the etch, this procedure removes about the topmost 14 nm of the polymeric material. Note that the same spot was imaged with SFM before (Figure 4a) and after etching (Figure 4b). Before etching terrace S_{PL} exhibits an array of protrusions, while no significant roughness is detected on terrace M_{PL}. After the etch, the protrusions on terrace S_{PL} have turned into depressions while terrace M_{PL} now exhibits an array of protrusions. We have determined the etching rates for the three components in a separate experiment[22,23] and found that the B and M blocks are etched twice as fast as the S block. Therefore, we can assign the continuous phase remaining after the etch on terrace S_{PL} as PS. The same holds for the protrusions formed on M_{PL} during the etch. To further distinguish between PB and PMMA, we have

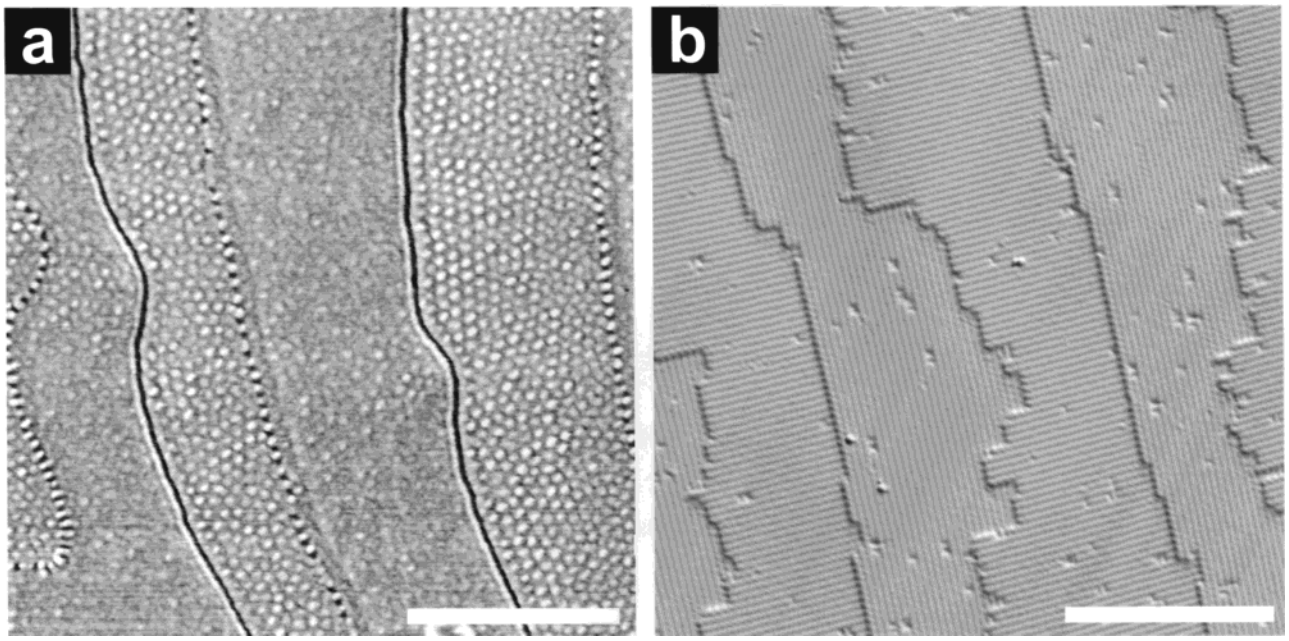

Figure 3. (a) TappingMode SFM phase image of a SBM[162] film showing the two different kinds of terraces at the free surface. Scale bar: 1 μm. (b) Scanning tunneling microscopy image of a stepped Si(100) surface forming a (2 × 1) surface reconstruction (courtesy of M. G. Lagally, University of Wisconsin, Madison). The different orientations of neighboring terraces are clearly visible. Scale bar: 5 nm.

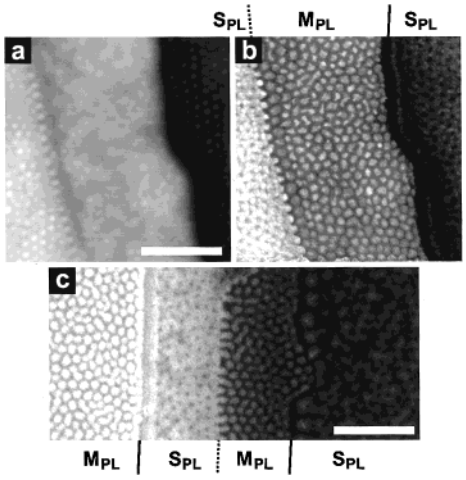

Figure 4. SFM height images of a SBM[162] film before (a) and after (b) etching with RF plasma. (c) shows a SEM image of a RuO_4-stained SBM[162] film. The dark regions correspond to PMMA rich areas. Scale bars: 1 μm.

Figure 5. Schematic model of the near surface morphology of SBM[162] (see text for explanation).

treated the films with RuO_4, which is known to selectively stain the PB and PS blocks. The samples were then investigated with a field emission SEM (Figure 4c). Under the employed imaging conditions the stained regions appear bright in the SEM images. Therefore, the dark areas can be assigned to M. From Figure 4c, we conclude that on terrace M_{PL} we have a continuous matrix of M, whereas on S_{PL}, isolated M domains are present.

Summarizing the results discussed so far, the following picture evolves. The bulk of the thin film exhibits a lamellar structure with the lamellae being aligned parallel to the film by virtue of interactions with the substrate (cross sectional TEM). The film develops "quantized" thicknesses, which are found to be integer multiples of half the lamellar spacing $L_{0,film}$ (SFM height images). Two different surface terminations of the lamellar structure are observed (M_{PL} and S_{PL}), which strictly alternate between neighboring terraces (SFM phase images). Terrace M_{PL} consists of isolated PS microdomains (SFM and etching) in a continuous matrix of PMMA (SEM and staining), while terrace S_{PL} is characterized by PMMA domains (SEM and staining) in a continuous matrix of PS (SFM and etching). In other words, terrace M_{PL} can be looked at as a perforated PMMA lamella with PS inclusions and vice versa for terrace S_{PL}. This finding led us to the notations M_{PL} and S_{PL}, respectively.

To visualize the potential structure of our films, Figure 5 shows a model comprising all the experimental results. In addition, the model allows for the fact that from the three components of our triblock copolymer, the PB middle block has the lowest surface energy. Therefore, we expect the surface to be covered homogeneously by a thin PB layer. In contrast to the ideal surface, which would be terminated with a PS block, the polymer rearranges, folding back the S chains into the adjacent M domain and thereby giving way to PB to cover the surface. Below this thin PB layer, the near surface structure is a continuous layer of PMMA perforated by isolated PS microdomains (M_{PL}). Accordingly, if a lamella would ideally terminate with PMMA, the respective process leads to a perforated layer of PS including isolated M microdomains. In both cases, a continuous layer of PB can cover the surface. The model

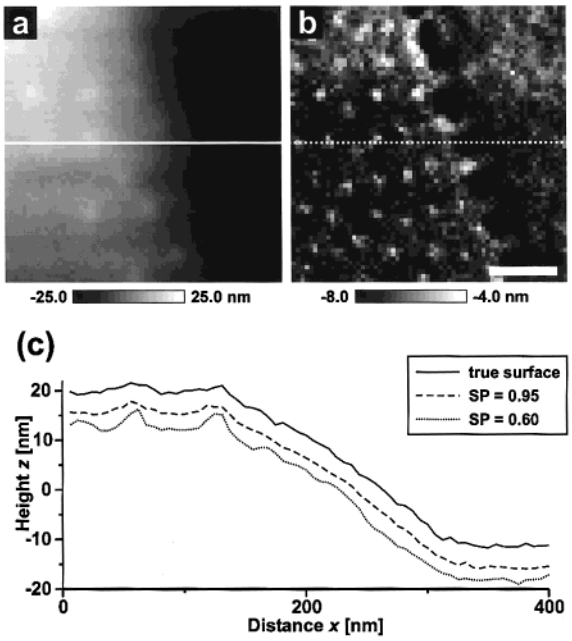

Figure 6. SFM images of a step from a S_{PL} terrace down to a M_{PL} terrace (from left to right): (a) image of the true surface; (b) image of the indentation with an amplitude set point of 0.6. It is the difference between the true surface image shown in part a and the height image taken at a set point of 0.6; scale bar: 100 nm. (c) Profiles of the true surface shown in part a and of height images determined from amplitude/phase vs distance curves for set points of 0.95 and 0.6. Tapping with a set point of 0.95 is usually called "soft tapping" . Note that there is no height offset between the three curves.

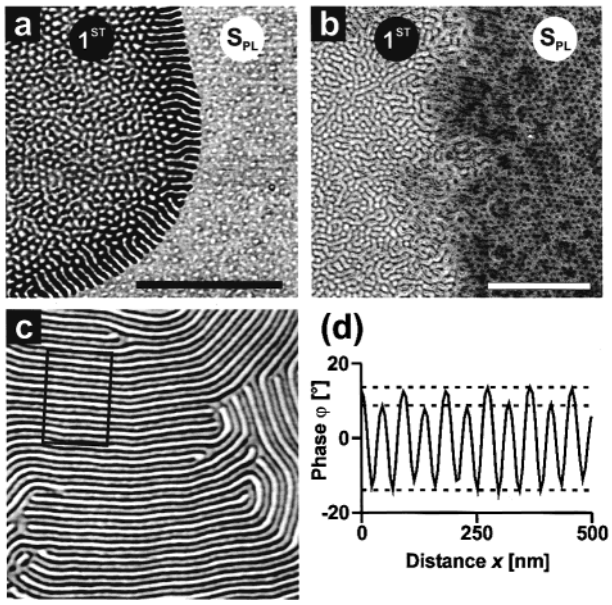

Figure 7. (a) TappingMode SFM phase image of an SBM[162] film. It shows the step between the first terrace and the neighboring S_{PL} terrace. (b) SEM image (RuO_4 stained) of a step between the first terrace and the neighboring S_{PL} terrace. (c) TappingMode SFM phase image of the stripe pattern appearing in regions with a film thickness of $t_{film} \approx 18$ nm. (d) Profile of the phase signal averaged along the short side of the boxed area in Figure 4c. The dotted lines are a guide to the eye.

explains both the existence of two different terminations which strictly alternate between neighboring terraces as well as the observation that the step heights H_{step} amount to only about half the lamellar spacing $L_{0,film}$ in the bulk of the film.

The existence of a homogeneous layer of polybutadiene on the surface of both S_{PL} and M_{PL} is—although expected in terms of surface energy—difficult to establish experimentally. We can get indirect evidence, however, by quantitative measurements of the indentation depths of the SFM tip during TappingMode imaging. As both PS and PMMA are glassy solids at room temperature, the SFM tip can indent only by small amounts under the typical imaging conditions. PB, on the other hand, is easily indented by several nanometers under typical imaging conditions, since it is a rubbery liquid at room temperature. SFM TappingMode height images of surfaces with a laterally varying stiffness do not necessarily represent the topography of the surface but are complex superpositions of both true surface topography and lateral variations in the indentation depth of the tip. Following a protocol devised by Knoll et al.,[24] we therefore have determined both an image of the true sample surface (Figure 6a) and of the absolute indentation depth at a set point of 0.6 (Figure 6b). The images consist of 64 × 64 data points, each of which is calculated from an entire amplitude/phase vs distance curve taken at the respective location. In Figure 6c, three line scans taken at different set points are shown. All heights are in absolute values. Indeed, the indentation of the tip is much higher than on a pure PS or PMMA surface. It is comparable to what was found on the surfaces of thin films of polystyrene-*block*-polybutadiene-*block*-polystyrene (SBS) exhibiting PS cylinders in a PB matrix.[24] Here, as well, the hard PS domains are covered with a continuous, soft PB layer. Our data therefore corroborate the presence of a continuous PB layer covering both surface terminations M_{PL} and S_{PL} found on the SBM surface.

In the thinnest regions of the film, yet another surface pattern is observed. This can be seen in the bottom of Figure 2 (middle part). Parts a and b of Figure 7 show higher magnification images of the boundary between this layer and the neighboring S_{PL} terrace. This pattern has the highest contrast in the SFM phase image. The most distinguished features are the stripelike domains oriented perpendicular to the boundary with the neighboring terrace.[25] We note that we have used this particular boundary structure to unambiguously identify the "layer number" both in the SFM and in the SEM experiments referred to above in order to assign S_{PL} and M_{PL} in the images taken by the two different techniques. We also note that in some of our experiments, this particular boundary pattern was found to extend over rather larger lateral areas. This can be seen in Figure 7c, which shows an SFM phase image of an area of thickness 18 ± 2 nm. A cross section through the phase image (Figure 7d) reveals that all three blocks are arranged in a stripe like fashion which may best be described as a perpendicular lamella. Although this particular structure may be of interest in the context of nanopatterning applications, we shall not discuss it in any further detail since this is not a surface reconstruction but an effect of confinement and shall be discussed elsewhere.

3.2. Effect of Block Copolymer Molecular Weight. SBM[54]. So far our discussion concerned the SBM[162] triblock copolymer only. We have performed similar experiments on thin films of the lower molecular weight SBM[54] triblock copolymer (Figure 8). This material shows qualitatively the same behavior, while all characteristic lengths, L_0, $L_{0,film}$, *and* H_{step}, as well as the

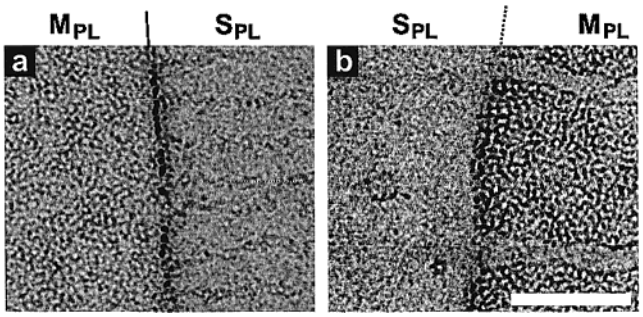

Figure 8. (a, b) TappingMode SFM phase images of a SBM[54] film. They show, from left to right, a step from an M_{PL} terrace down to an S_{PL} terrace (a) and a step from an S_{PL} terrace down to an M_{PL} terrace (b). Scale bar: 500 nm.

in-plane characteristic spacing, are considerably smaller. The step heights are again significantly smaller than the lamellar period found in bulk samples. In the SFM phase images, we observe a weaker contrast between the different blocks. This may be attributed in part to the smaller lateral domain size. In addition, PS and PMMA will be less incompatible at this rather small molecular weight. In consequence, the PS/PMMA interfaces are considerably wider and the two polymers exhibit weaker segregation. However, qualitatively the same features are observed: Two different surface terminations are found to alternate between neighboring terraces, and two types of steps can be identified on top of an otherwise lamellar structure.

Aside from the differences in molecular weight, SBM[54] exhibits an almost perfectly symmetric composition ($\phi_{PS} = 0.34$, $\phi_{PB} = 0.37$, $\phi_{PMMA} = 0.29$), while in SBM[162] the PB block is significantly larger than the PMMA block ($\phi_{PS} = 0.33$, $\phi_{PB} = 0.47$, $\phi_{PMMA} = 0.20$). The observation that SBM[54] shows qualitatively the same surface behavior therefore clearly indicates that the effects described above for the higher molecular weight material *are not due* to its asymmetric composition.

3.3. Role of Molecular Topology. BSM. In the above discussion, we have identified the lower surface energy of the PB middle block as the driving force for the rearrangement of the near-surface microdomain structure of SBM thin films. To test this hypothesis, we have extended our investigations to thin films of BSM triblock copolymers, where the low surface energy PB block has been moved from the middle to one of the ends of the block copolymer. In this case, the lamellar structure should extend throughout the entire film, and we expect a lateral homogeneous film surface. We start again with the cross sectional TEM image (Figure 1b), which shows a lamellar microdomain morphology. Since we only stain the PB block by RuO_4 and PS and PMMA domains are no longer separated by PB, we cannot distinguish all three blocks. However, the alignment of the lamellae parallel to the plane of the film is clearly visible. We also find a certain shrinkage of the films perpendicular to the lamellae; i.e., the lamellar period $L_{0,film}$ is again smaller than the bulk value L_0.[19] SFM height images show regions of well-defined thickness separated by steps of height H_{step}. To determine the absolute thickness of the different regions with SFM, we applied a scratch to the film, which reached down to the substrate surface (Figure 9a). From the height profiles obtained this way (Figure 9c), we find that $H_{step} \approx L_{0,film}$ for all but the first steps. The first step, i.e., the thickness of the thinnest regions of the film amount to about $^1/_2 L_{0,film}$. Again the absolute values of

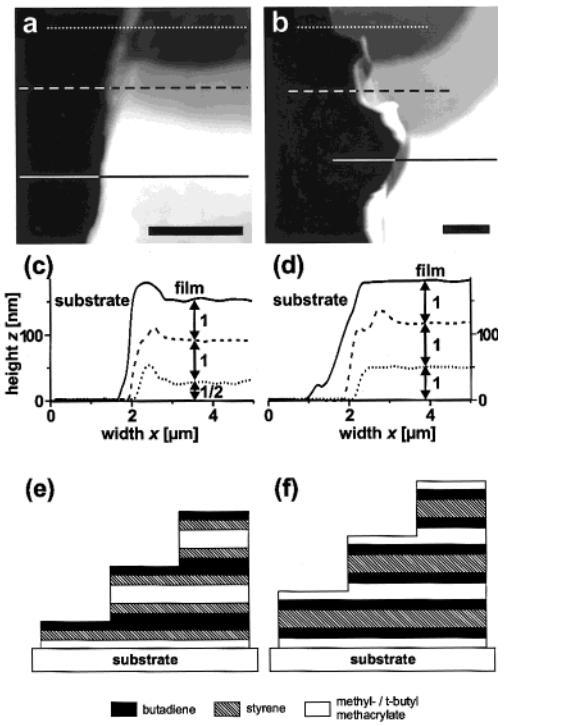

Figure 9. SFM height images of a scratch (at the left side of the images) in a BSM (a) and an SBT film (b). Parts c and d show height profiles of the corresponding lines in parts a and b, respectively. Parts e and f are schematic models of BSM (e) and SBT (f) films. Scale bars: 2 μm.

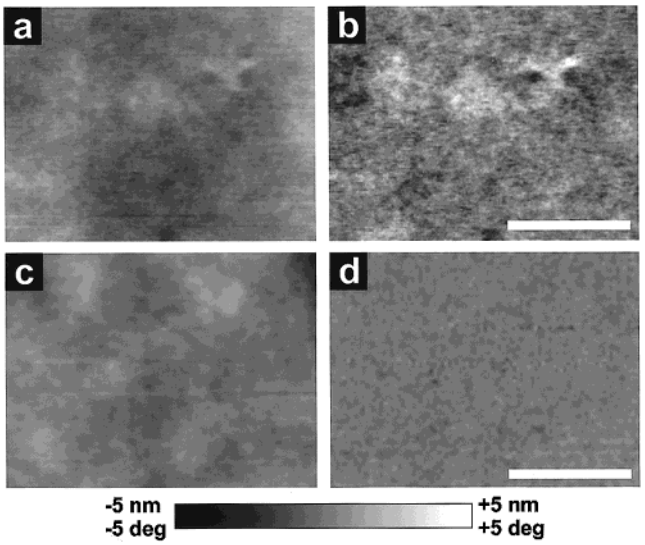

Figure 10. TappingMode SFM height (left) and phase images (right) of the free surface of BSM (a, b) and SBT (c, d), respectively. Scale bars: 400 nm.

film thickness H_{film} vary due to differences in preparation, but the relative values all follow the relation $H_{film} \approx (n + {}^1/_2)\, L_{0,film}$ with $n = 0, 1, 2, \ldots$. Closer inspection of the surfaces by SFM imaging did not reveal any lateral structure on the terraces (Figure 10, parts a and b).

The results on BSM resemble the well-known behavior of lamella forming diblock copolymer thin films under asymmetric wetting conditions, i.e., when one of the blocks preferentially wets the substrate while the other preferentially wets the surface of the film.[9] This behavior is found, e.g., for PS-*block*-PMMA diblock copolymers on polar substrates: Having a lower surface

energy, PS accumulates at the free surface while PMMA is attracted to the polar substrate. Consequently, the smallest "quantized" value of film thickness compatible with these boundary conditions is $^1/_2L_0$. Thicker films will tend to form $(n + {}^1/_2)$ multiples of L_0. In BSM, the B block has the lowest surface energy while the M block is attracted to the substrate. The S middle block can be considered "neutral" with respect to the boundary surfaces and therefore does not interfere with the lamellar structure in the thin film.

3.4. Strength of the Surface Field. SBT. We turn back to the surface reconstruction observed in the SBM system, where we have identified the gain in surface energy as the driving force for the formation of a different near surface structure. One has to realize, though, that the proposed "backfolding" of the PS and PMMA blocks into the topmost PMMA and PS lamellae, respectively, will lead to an increase in free energy, both by unfavorable chain conformations (entropic contribution) and by the creation of additional PS/PMMA interfaces (enthalpic contribution). In the case of SBM, this cost in free energy seems to be more than compensated for by the gain in surface free energy realized by the exposition of PB to the free surface.

This is not necessarily the case. To demonstrate the competition between the different contributions to the free energy, we have studied thin films of SBT as well. The incompatibility between the two end blocks PtBMA and PS is larger than in the case of PS and PMMA.[19] In addition, the surface energy difference between the middle block PB and the lower surface energy end block PtBMA is smaller than in the case of SBM.[26] In consequence, one may expect a different surface behavior. We again start our discussion with the cross sectional TEM results (Figure 1c). A lamellar morphology is observed as in the two preceding cases. The lamellae are aligned parallel to the plane of the film. Also a terraced film topography is formed. In contrast to both preceding cases, however, SFM investigation of the height profiles (Figure 9, parts b and d) show that the quantized values of film thickness are *integer* multiples of the lamellar spacing, i.e., $H_{\text{film}} \approx nL_{0,\text{film}}$ with $n = 1, 2, 3, \ldots$. As detected by SFM topography (Figure 10c) and phase imaging (Figure 10d), the surfaces of the films do not exhibit any lateral features.

This result is comparable to what is known for lamella forming diblock copolymers under symmetric wetting conditions, i.e., when the same block preferentially wets both interfaces.[20] The increased interfacial tension between PS and PtBMA together with a decreased driving force (i.e., a smaller surface energy difference between PtBMA and PB) prohibits the formation of a lateral surface structure, which would allow the lower surface energy component *B* to be exposed at the free surface. A comparison of the behavior of SBM and SBT indicates that a subtle balance between the different contributions to the free energy of the system determines whether the termination of the bulk structure at the free surface is "ideal" or whether a reconstruction of the near-surface structure is energetically favorable.

4. Discussion

The experiments described above clearly show that the near-surface structure of a block copolymer sample can deviate from the bulk structure by formation of a surface reconstruction. By comparing the behavior of different ABC triblock copolymers, we have identified

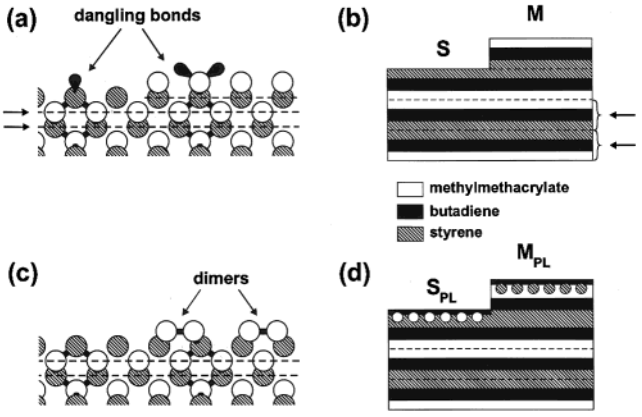

Figure 11. Schematic model of ideal (left) and reconstructed surfaces (right) of Si(100) (a, c) and SBM (b, d). The arrows in parts a and b indicate the nonequivalent layers.

the gain in surface free energy as the driving force for this surface reconstruction. Moreover, we have given evidence that the gain in surface free energy must be large enough to balance other (positive) contributions to the free energy related to the deviation from the bulk structure in order for a surface reconstruction to be formed. In the following, we shall briefly recall the concept of surface reconstructions as introduced in classical surface science and identify some similarities and differences between the different classes of materials. We shall then propose a general nomenclature for block copolymer surface reconstructions. Finally, we shall discuss the experimental conditions required for a successful study of block copolymer surface structures.

4.1. Similarity to Surface Reconstructions of Inorganic Crystals. We start our discussion by considering a perfect single crystal, which is terminated along one of its crystal planes by a surface. If the crystal structure of the respective planes remains unchanged all the way to the surface layer, one often refers to this termination as the *ideal surface* of the crystal. However, quite often the atomic layers near the surface do not exhibit the same structure as the respective bulk crystal planes. Because of the absence of neighboring atoms, the distribution of electron density and atomic nuclei experience a potential considerable different from the bulk. As a consequence, a different spatial distribution of electron density and nuclei may result, representing the lowest free energy state of the system. In the case of so-called *surface relaxations*, the in-plane structure of the surface layers remains unchanged and only the layer spacing is affected by the presence of the surface. Often, however, the in-plane structure is changed as well. This situation is referred to as a *surface reconstruction*. While many metal surfaces exhibit surface relaxations only, covalently bound materials often exhibit complex surface reconstructions.

The Si(100)−(2 × 1) surface represents a well-known example for a surface reconstruction. In the case of the ideal Si(100) surface, two-half-filled electronic orbitals (so-called *dangling bonds*) would extend from each surface atom into free space (Figure 11a). This state is characterized by a rather high surface energy. A lower free energy is reached by the formation of atomic dimers in the surface layer, which cuts the number of dangling bonds in half and thereby considerably reduces the surface energy. Different microscopic models have been proposed for the detailed structure of the Si(100)−(2 × 1) surface reconstruction, and a discussion of them

would be beyond the scope of the present article.[27−29] We only note that the formation of dimers breaks the 4-fold symmetry of the (100) lattice plane of the cubic diamond lattice and leaves the surface with only 2-fold symmetry. This is clearly revealed by scanning tunneling microscopy images[29] of the reconstructed surface as shown in Figure 3b. The image has been taken on a stepped surface. Each of the terraces exhibits straight lines resulting from rows of Si dimers. Quite interestingly, the orientation of these dimer rows rotates by 90° between successive terraces. Therefore, the stepped surface is characterized by two nonequivalent terminations, which strictly alternate between successive terraces. Along with the orientation of the dimer rows, the shape of the monatomic steps alternates as well between rather straight steps and meandering steps, the latter being rich in kinks.

The alternation between two different dimer row orientations results from the particular crystal structure of silicon. We may view the diamond lattice as a stack of (100) planes. As we move perpendicular to this stack, the orientation of the two bonds connecting between atoms in adjacent (100) layers rotates by 90° from layer to layer. Therefore, the orientation of the Si dimers at the surface rotates by 90° between adjacent terraces on a stepped surface as well. We may therefore envisage the diamond lattice as a alternating stack of two nonequivalent (100) layers, which have different surface properties, i.e., different orientations of the Si dimer rows. We note that the two layers are transformed into each other by reflection at a mirror plane along (100).

The observations on the SBM surfaces closely resemble the situation of the Si(100) surface: The near-surface region exhibits a structure different from the *ideal* case, which would be a laterally homogeneous termination by one of the end blocks of the block copolymer. Moreover, two different terminations are observed, which strictly alternate between adjacent terraces on a stepped block copolymer surface. Finally, the shape of the steps limiting the terraces alternates between two different possibilities as well. Similar to the case of the diamond lattice, the bulk structure of a lamellar ABC triblock copolymer can also been described as an alternating stack of two nonequivalent layers, i.e., ABC and CBA. Also the two layers are transformed into each other via reflection at a mirror plane along the layers. While equivalent in the bulk, these two layers will have different surface properties, as they lead to ideal surfaces terminated with one or the other end block.

The structure of a classical crystal is described by the periodic spatial arrangement of electron density and *pointlike* nuclei. Therefore, its symmetry belongs to the class of *point groups*. The microdomain structure of a block copolymer on the other hand is described by the density of its components (S, B, and M in the case of SBM) and a region with an increased density of one component is called a microdomain. Microdomains can form spheres, cylinders, lamellae or more complex shapes, which self-assemble into regular periodic structures resembling crystal like order. However, as cylinders and lamellae exhibit (partial) continuous translational symmetry, the corresponding bulk microdomain structures belong to the more general class of *space groups*. (Smectic and columnar phases of liquid crystals exhibit a similar symmetry.)

The lateral order within the layers of the bulk structure is different for the two materials: Si is a classical crystal with 2D lattice symmetry within its (100) plane, while the SBM bulk structure is lamellar with continuous 2-dimensional translational symmetry (Euclidian symmetry) within the lamellae. In both cases the symmetry of the reconstructed surface is lowered with respect to the ideal surface, however in very different ways. In the case of the Si(100) surface the size of the unit cell of the 2D surface lattice doubles. In the case of SBM, the Euclidian symmetry is broken. We emphasize the fact that in both cases a laterally homogeneous boundary imposed in the direction *perpendicular* to the layer breaks the *in-plane* symmetry of the ideal surfaces. This indicates that all three spatial coordinates are coupled on an underlying microscopic scale. This coupling is due to the 3-dimensional nature of the underlying elements (atoms in one case and polymer molecules in the other). The same phenomenon is found in other fields of physics (e.g., high energy physics), where the type of symmetry breaking can reveal properties of underlying (invisible) microscopic particles and processes.

4.2. Nomenclature. The notation used for crystal surfaces can also be applied to surfaces and surface reconstructions of block copolymers (Table 2). This further illustrates the analogy between both classes of materials. Usually first the material and its crystal structure is identified, for instance, α-Sn, 6H-SiC, or GaAs. For denoting the bulk microdomain structures of block copolymers we have followed the notation of Stadler et al.[18] (To focus on the microdomain structures, we have not denoted the stoichiometry and the total molecular weight of the block copolymers in Table 2.) For ABC triblock copolymers a two-letter prefix is used to indicate the shape of the two main structural elements. For instance, *ll* denotes the S and M lamellae in the SBM triblock copolymer that we have studied. In the case of the SBM triblock copolymer studied by Stocker et al.,[14] the bulk structure is referred to as "lamellar−spherical"[18] which is denoted by the prefix *ls*. The next part of the notation identifies the surface and its orientation, for instance, (100) or (111). Miller indices can also be used to denote planes (and surfaces) in block copolymer microdomain structures. However, as single crystals of block copolymers are rare, there is no general agreement on the assignment of unit cells for the various microdomain structures, in particular for the rather new ABC triblock copolymers. Another difficulty is that many microdomain structures, in particular cylinders and lamellae, have continuous symmetry. Although it is straightforward to define unit cells also for these systems, the definition is not unique. To avoid this problem, we have used the "natural" block copolymer language to specify lattice planes and surfaces in cylinder and lamella forming systems. In a lamellar system, the lattice planes (and surfaces) parallel and perpendicular to the lamellae are well-defined and we have denoted them as $L_{||}$ and $L_{\perp}$, respectively. In a polar system different surfaces with the same Miller indices are denoted with a suffix, for instance, GaAs(111)*A*.[30] Analogous to this notation we have denoted the two different ideal surfaces of lamella forming SBM with a suffix which indicates the component at the free surface. For instance, *ll*-SBM($L_{||}$)M denotes the ideal M-covered surface parallel to a lamella. In analogy to the notation used for inorganic crystals,

Table 2. Examples of Ideal Surfaces and Surface Reconstructions (See Text for Explanation)

material (surface)	surface reconstruction	notation	acronym	experiment	theory[a]
		(a) Inorganic Crystals			
α-Sn					
6H-SiC					
GaAs(111)	ideal A surface	GaAs(111)*A*		30	
Si(100)	(2 × 1) buckling row	Si(100)−(2 × 1)		28, 29	
Si(111)	(7 × 7)	Si(111)−(7 × 7)		7	
		(b) Block Copolymers			
c-SBS($C_\perp$)	ideal surface	*c*-SBS($C_\perp$)	$C_\perp$	32, 39,[b] 40[b]	32, 41−45
c-SBS($C_{||}$)	ideal surface	*c*-SBS($C_{||}$)	$C_{||}$	24, 32, 39,[b] 40,[b] 46	32, 41−45
c-SBS($C_{||}$)	perforated lamella	*c*-SBS($C_{||}$)-PL	PL	34,[b] 32	32, 42, 43, 45
c-AB($C_{||}$)	lamella	*c*-AB($C_{||}$)-L	L	34[b]	32, 41−43
c-AB($C_{||}$)	wetting layer	*c*-AB($C_{||}$)-W	W	33[b]	32, 41−43, 45
ll-SBM($L_{||}$)	ideal M surface	*ll*-SBM($L_{||}$)M	M		
ll-SBM($L_{||}$)	perforated M lamella	*ll*-SBM($L_{||}$)M-PL	M_{PL}	this work	
ll-SBM($L_{||}$)	perforated S lamella	*ll*-SBM($L_{||}$)S−PL	S_{PL}	this work	
ls-SBM($L_\perp$)	missing row	*ls*-SBM($L_\perp$)−(2 × 1)		14	
		(c) Block Copolymers (Hybrid Structures)			
c-SBS($C_{||}$)	cylinders with necks	*c*-SBS($C_{||}$)-necks		45	47
c-SB	PL and spheres			48[b]	47

[a] Only in ref 32 are cylinder-forming triblock copolymers studied; all other studies investigate diblock copolymers. [b] Work on cylinder-forming diblock copolymers.

the type of surface reconstruction is added to the "name" of the ideal surface. For example, the full name of the M_{PL} perforated lamella reconstruction of a surface parallel to a bulk lamella is *ll*-SBM($L_{||}$)M-PL. With this notation also other surface structures can be described (see Table 2). For instance, Stocker et al.[14] have reported at the surface of SBM a striped surface structure with twice the period of the lamellar bulk structure and have interpreted it as a missing row surface reconstruction. Analogous to crystal surfaces, the period doubling along (only) one lattice direction is denoted as a (2 × 1) reconstruction.

4.3. Experimental Conditions for Block Copolymer Surface Studies. Similar to the situation for inorganic crystals, most impurities tend to be surface active and enrich in the near-surface region when the sample is driven toward thermal equilibrium. Therefore, the actual surface structure may easily be dominated by even smallest amounts of impurities present in the bulk of the material. Indeed, complex block copolymers often contain considerable amounts of residues of the synthesis process, such as homopolymers, other (lower generation) block copolymers, oligomers or other additives. While in the case of many classical crystals, the bulk material can be depleted from impurities by iterative cycles of thermal annealing and surface cleaning (e.g., by ion sputtering), no such cleaning procedures are established for block copolymer surfaces. Therefore, bulk pieces of block copolymer material are questionable candidates for surface studies. Indeed, transmission electron studies of the near-surface region of diblock copolymer samples have revealed significant deviations from the bulk structure, which were attributed to accumulation of impurities (Figure 12).[31]

Figure 12. Cross-sectional TEM micrograph (OsO_4 stained) of the near-surface morphology of an SB 80/80 diblock copolymer sample showing the complex morphology with a contaminant thought to be a fully polymerized PS block with varying lengths of PB. The external surface has been marked with a layer of gold. The normal lamellar structure is ∼10 μm below the surface. Reprinted with permission from ref 31. Copyright 1992 Massachusetts Institute of Technology. Courtesy of E. L. Thomas, Massachusetts Institute of Technology, Cambridge, MA.

In the case of classical surface science, two alternative routes have been devised for cases in which clean surfaces cannot be achieved by successive annealing and surface cleaning. At first, cleavage of bulk pieces of material can be used to create "clean" surfaces. Since a single crystal typically cleaves along a preferred low-index crystallographic plane, a surface of well-defined crystallographic orientation is created. However, for a study of the equilibrium structure these surfaces will have to be annealed as well and a compromise has to be found concerning the annealing conditions, to avoid a significant amount of bulk impurities migrating to the newly created surface. Second, thin films of the material of interest can be prepared on suitable substrates again creating a clean surface. Here, the total amount of material (including impurities) is purposely kept small and the problem of impurities accumulation at the

surface is less severe. However, the film thickness has to be chosen large enough in order to ensure that the (bulk) crystal structure of interest is actually formed underneath the surface. Otherwise, confinement effects may dominate the entire structure of the film and the results will not reflect the surface properties of a bulk piece of the same material.

For block copolymers, the same two routes are in principle accessible. Instead of cleavage, a new surface may be created within the bulk of a sample by (cryo) microtoming and subsequent (short) annealing. As in the case of classical crystals, one has to ensure that the annealing is sufficient to create the equilibrium surface structure, however, does not allow significant impurity migration. In contrast to the favorable situation of classical single crystals, the newly created surface will not be a low index crystallographic plane but will rather cut through a variety of grains at arbitrary orientation. Large scale alignment of the block copolymer microdomain structure in external fields prior to cutting may be a successful approach.

Alternatively, the surfaces of thin films may be investigated. Here, one has to ensure that the "bulk" of the films is thick enough to form the structure expected for the bulk block copolymer material. As in the case of classical crystals, confinement effects may dominate the microdomain structure in very thin films.[32] In contrast, though, the characteristic film thickness above which bulk behavior is to be expected will be significantly larger in the case of block copolymers due to the inherent large molecular length scales. If the film thickness is kept small enough, though, the interactions with the supporting substrate can lead to microdomain alignment and a free surface of well-defined crystallographic orientation may be created. In any case, the "bulk morphology" of the thin film has to be experimentally established (see Figure 1) before potential surface reconstructions can be identified.

4.4. Comparison to Earlier Experimental Results. The concept of block copolymer surface reconstructions was first introduced in a paper by Stocker et al.,[14] who investigated the surface structure of an SBM triblock copolymer bulk sample with a rather small volume fraction of the B middle block and about equal volume fractions of the S and M end blocks. In the bulk, the material formed lamellae of S and M with B spheres located at the S/M interfaces. At the surface, indications of a perpendicular orientation of the lamellae were observed and the B spheres were visualized by TappingMode SFM by virtue of their different mechanical properties. The SFM results indicated an in-plane periodicity different from the bulk periodicity determined by TEM. This difference was attributed to a surface reconstruction.

Other studies have reported thin film structures different from the respective bulk structures, which can also be attributed to surface reconstructions. Indeed, in cylinder-forming block copolymer systems, a variety of thin film structures has been reported on, including a laterally homogeneous wetting layer,[33] spherical microdomains,[34] and a perforated lamella.[34] Systematic studies of the thin film phase behavior as a function of both surface interaction and film thickness have recently been performed both experimentally and by dynamic density functional calculations.[32] These studies have revealed that in thin films both surface reconstructions and confinement play a role and the resulting equilibrium structures are determined by the interplay of the two.

Other studies have reported on particular thin film structures such as the so-called hybrid structure in lamellar-forming diblock copolymer thin films[35] and cylinders exhibiting necks toward the free surface in cylinder-forming block copolymers.[23] In the former case, asymmetric wetting conditions were shown to lead to a parallel alignment of the lamellae at the substrate interface, while a perpendicular orientation of the lamellae was found at the free surface. This finding, however, may rather be attributed to the observation of two grains exhibiting the bulk structure, divided by a planar grain boundary stabilized by surface interactions. The observation of cylinders with necks may be described in similar terms.

Other, more complex thin film structures have recently been described for ABC triblock copolymer thin films.[36,37] Here, however, it remains unclear to what extend thermal equilibrium has been reached during film preparation. Further studies will be needed to unambiguously classify the respective structures in the framework provided here.

5. Conclusion

We have shown that differences in surface energy between the different constituent materials of a block copolymer can lead to deviations of the near surface structure from the bulk structure, so-called *surface reconstructions*. Despite the fundamental differences between the materials, the type of order and symmetry, and the length scales, these surface reconstructions exhibit many similarities to the well-known surface behavior of classical crystals. This finding indicates that the concept of surface reconstruction is not limited to classical crystals but can appear in similar ways for other kinds of ordered materials as well. For the particular case of block copolymers, the concept of surface reconstructions and the clear distinction between surface reconstructions and confinement effects can lead to a deeper understanding of the underlying physics determining block copolymer thin film structures.

Acknowledgment. The authors appreciate helpful discussions with V. Abetz, T. Goldacker, and E. L. Thomas. We are grateful to M. G. Lagally and to E. L. Thomas for providing Figures 3b and 12, respectively. We acknowledge the contributions of M. Konrad and S. Ludwigs at the beginning of this work and C. Abetz and C. Kunert for electron microscopy. This work was financially supported by the Deutsche Forschungsgemeinschaft (SFB 481).

References and Notes

(1) Bates, F. S.; Fredrickson, G. H. *Phys. Today* **1999**, *52*, 32.
(2) Witten, T. A. *Rev. Mod. Phys.* **1999**, *71*, S367.
(3) Seul, M.; Andelman, D. *Science* **1995**, *267*, 476.
(4) Tsori, Y.; Andelman, D. *J. Chem. Phys.* **2001**, *115*, 1970.
(5) Hashimoto, T.; Bodycomb, J.; Funaki, Y.; Kimishima, K. *Macromolecules* **1999**, *32*, 2.
(6) Zangwill, A. *Physics at Surfaces*; Cambridge University Press, Cambridge, England, 1988.
(7) Binnig, G.; Rohrer, H.; Gerber, C.; Weibel, E. *Phys. Rev. Lett.* **1983**, *50*, 120.
(8) Ragosti, A. K.; Pierre, L. E. S. *J. Colloid Interface Sci.* **1969**, *31*, 168.
(9) Anastasiadis, S. H.; Russell, T. P.; Satija, S. K.; Majkrzak, C. F. *Phys. Rev. Lett.* **1989**, *62*, 1852.

(10) Krausch, G. *Mater. Sci. Eng. Rep.* **1995**, *14*, 1.
(11) Fasolka, M. J.; Mayes, A. M. *Ann. Rev. Mat. Res.* **2001**, *31*, 323.
(12) Pickett, G. T.; Balazs, A. C. *Macromol. Theory Simul.* **1998**, *7*, 249.
(13) Chen, H.-Y.; Fredrickson, G. H. *J. Chem. Phys.* **2002**, *116*, 1137.
(14) Stocker, W.; Beckmann, J.; Stadler, R.; Rabe, J. P. *Macromolecules* **1996**, *29*, 7502.
(15) Elbs, H.; Fukunaga, K.; Sauer, G.; Stadler, R.; Magerle, R.; Krausch, G. *Macromolecules* **1999**, *32*, 1204.
(16) Fukunaga, K.; Elbs, H.; Krausch, G. *Langmuir* **2000**, *16*, 3474.
(17) Rehse, N.; Knoll, A.; Konrad, M.; Magerle, R.; Krausch, G. *Phys. Rev. Lett.* **2001**, *87*, 035505.
(18) Stadler, R.; Auschra, C.; Beckmann, J.; Krappe, U.; Voigt-Martin, I.; Leibler, L. *Macromolecules* **1995**, *28*, 3080.
(19) Goldacker, T. Ph.D. Thesis, Universität Bayreuth, Bayreuth, Germany, 1999.
(20) Anastasiadis, S. H.; Russell, T. P.; Satija, S. K.; Majkrzak, C. F. *J. Chem. Phys.* **1990**, *92*, 5677.
(21) Brinkmann, S.; Stadler, R.; Thomas, E. L. *Macromolecules* **1998**, *31*, 6566.
(22) Konrad, M. Diploma Thesis, Universität Bayreuth, Bayreuth, Germany, 1999.
(23) Konrad, M.; Knoll, A.; Krausch, G.; Magerle, R. *Macromolecules* **2000**, *33*, 5518.
(24) Knoll, A.; Magerle, R.; Krausch, G. *Macromolecules* **2001**, *34*, 4159.
(25) A similar pattern has been observed at terrace edges with diblock copolymer films: Carvalho, B. L.; Thomas, E. L. *Phys. Rev. Lett.* **1994**, *73*, 3321.
(26) Mark, J. E. *Physical Properties of Polymers Handbook*; Woodbury: New York, 1996.
(27) Tromp, R. M.; Hamers, R. J.; Demuth, J. E. *Phys. Rev. Lett.* **1985**, *55*, 1303.
(28) Dijkamp, D.; Hoeven, A. J.; Loenen, E. J. v.; Lenssinck, J. M.; Dieleman, J. *Appl. Phys. Lett.* **1990**, *56*, 39.
(29) Swartzentruber, B. S.; Kitamura, N.; Lagally, M. G.; Webb, M. B. *Phys. Rev. B* **1993**, *47*, 13432.
(30) Ohtake, A.; Nakamura, J.; Komura, T.; Hanada, T.; Yao, T.; Kuramochi, H.; Ozeki, M. *Phys. Rev. B* **2001**, *64*, 045318.
(31) Schwark, D. W. Ph.D. Thesis, Massachusetts Institute of Technology, Cambridge, MA, 1992.
(32) Knoll, A.; Horvat, A.; Lyakhova, K. S.; Krausch, G.; Sevink, G. J. A.; Zvelindovsky, A. V.; Magerle, R. *Phys. Rev. Lett.* **2002**, *89*, 035501.
(33) Karim, A.; Singh, N.; Sikka, M.; Bates, F. S.; Dozier, W. D.; Felcher, G. P. *J. Chem. Phys.* **1994**, *100*, 1620.
(34) Radzilowski, L. H.; Carvalho, B. L.; Thomas, E. L. *J. Polym. Sci., B: Poly. Phys.* **1996**, *34*, 3081.
(35) Fasolka, M. J.; Banerjee, P.; Mayes, A. M.; Pickett, G.; Balasz, A. *Macromolecules* **2000**, *33*, 5702.
(36) Elbs, H.; Drummer, C.; Abetz, V.; Hadziioannou, G.; Krausch, G. *Macromolecules* **2001**, *34*, 7917.
(37) Elbs, H.; Drummer, C.; Abetz, V.; Krausch, G. *Macromolecules* **2002**, *35*, 5570.
(38) Breiner, U. Ph.D. Thesis, Universität Mainz, Mainz, Germany, 1996.
(39) Kim, G.; Libera, M. *Macromolecules* **1998**, *31*, 2569.
(40) Kim, G.; Libera, M. *Macromolecules* **1998**, *31*, 2670.
(41) Turner, M. S.; Rubinstein, M.; Marques, C. M. *Macromolecules* **1994**, *27*, 4986.
(42) Huinik, H. P.; Brokken-Zijp, J. C. M.; van Dijk, M. A. v.; Sevink, G. J. A. *J. Chem. Phys.* **2000**, *112*, 2452.
(43) Huinik, H. P.; van Dijk, M. A.; Brokken-Zijp, J. C. M.; Sevink, G. J. A. *Macromolecules* **2001**, *34*, 5325.
(44) Pereira, G. G. *Phys. Rev. E* **2001**, *63*, 061809.
(45) Wang, Q.; Nealy, P. F.; de Pablo, J. J. *Macromolecules* **2001**, *34*, 3458.
(46) van Dijk, M. A.; van den Berg, R. *Macromolecules* **1995**, *28*, 6773.
(47) Lyakhova, K. S.; Sevink, G. J. A.; Zvelindovsky, A. V.; Horvat, A.; Magerle, R. To be published.
(48) Harrison, C.; Park, M.; Chaikin, P. M.; Register, R. A.; Adamson, D. H.; Yao, N. *Macromolecules* **1998**, *31*, 2185.

MA021134V